

Radial velocity measurements of the pulsating zirconium star: LS IV–14°116^{*}

C. S. Jeffery^{1,2†}, A. Ahmad¹, Naslim, N.^{1,3}, W. Kerzendorf^{4,5}

¹*Armagh Observatory, College Hill, Armagh BT61 9DG, UK*

²*School of Physics, Trinity College Dublin, College Green, Dublin 2, Ireland*

³*Academia Sinica Institute of Astronomy and Astrophysics, Taipei 10617, Taiwan R.O.C*

⁴*Research School of Astronomy & Astrophysics, ANU College of Physical & Mathematical Sciences, Mount Stromlo Observatory, ACT 2611, Australia*

⁵*Dept of Astronomy and Astrophysics, University of Toronto, 50 St. George Street, Toronto, Ontario, Canada, M5S 3H4*

Accepted Received ...; in original form ...

ABSTRACT

The helium-rich hot subdwarf LSIV –14°116 shows remarkably high surface abundances of zirconium, yttrium, strontium, and germanium, indicative of strong chemical stratification in the photosphere. It also shows photometric behaviour indicative of non-radial g-mode pulsations, despite having surface properties inconsistent with any known pulsational instability zone. We have conducted a search for radial velocity variability. This has demonstrated that at least one photometric period is observable in several absorption lines as a radial velocity variation with a semi-amplitude in excess of 5 km s^{-1} . A correlation between line strength and pulsation amplitude provides evidence that the photosphere pulsates differentially. The ratio of light to velocity amplitude is too small to permit the largest amplitude oscillation to be radial.

Key words: asteroseismology,, stars: chemically peculiar, stars: subdwarf, stars: individual (LS IV–14°116), stars: pulsation

1 INTRODUCTION

The helium-rich hot subdwarf LSIV –14°116 is remarkable for several reasons. Its peculiarity was first recognised in a spectroscopic follow-up of UV-excess objects (Viton et al. 1991). Subsequent analyses confirmed the excess helium abundance and high effective temperature (T_{eff}), making it one of relatively few such stars (Ahmad & Jeffery 2003; Ahmad & Jeffery 2004), and the only one to show photometric variability (Ahmad & Jeffery 2005). Follow-up photometry confirmed the star to be a multi-periodic variable, almost certainly a non-radial g-mode oscillator (Jeffery 2011; Green et al. 2011) with a dominant pulsation signal at 1953 s ($=0.022 \text{ d}$) and weaker signals at 2620, 2872, 3582, 4260 and 5084 s. However LSIV –14°116 presents a problem in that its effective temperature and gravity are deemed inconsistent with domains known to be unstable to g-mode oscillations (Jeffery & Saio 2006, 2007; Green et al. 2011). A further surprise came with the discovery of superabundances (by $\sim 4 \text{ dex}$) of zirconium, yttrium, strontium, and, to a lesser extent, germanium (Naslim et al. 2011). It has been argued that these could be associated with a dynamical self-stratification of the photosphere as a young subdwarf contracts towards the extreme horizontal branch (Naslim et al. 2013), suggesting that LSIV –14°116 is a proto-sdB star which will eventually develop a helium-poor

atmosphere, and prompting speculation that the oscillations might represent the first known case of ϵ -driven¹ pulsation (Miller Bertolami et al. 2011, 2012). Meanwhile, the exotic surface chemistry suggested that, as in some Bp(He) stars (Townsend et al. 2005), magnetic activity might be responsible for the variability (Naslim et al. 2011), a speculation quite delicately dismantled by Green et al. (2011).

Whilst LSIV –14°116 presents conundra in terms of the driving mechanism for the pulsation, its surface composition and its actual effective temperature (Green et al. 2011), more basic data are also required. First, many hot subdwarfs are known to be members of binaries, providing at least three mechanisms for the removal of surface layers necessary for evolution to the extreme horizontal branch. LSIV –14°116 is a very slow rotator (Naslim et al. 2011); would radial-velocity measurements show it to be a binary? Second, if light variations are due to pulsation (and not magnetic activity), surface motion should be detectable in radial-velocity data at periods equal to the light variations. Such measurements could ultimately provide direct radius measurements or mode identifications using techniques similar to the Baade-Wesselink method (Stamford & Watson

¹ *i.e.* driven by instability in a nuclear burning zone.

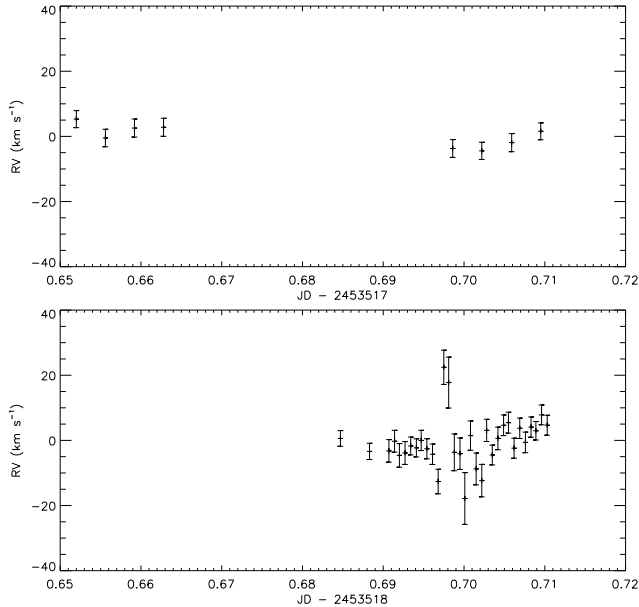


Figure 1. Relative radial velocities for LS IV $-14^\circ 116$ obtained with WHT/ISIS on 2005 May 27 and 28.

1981). Third, Naslim et al. (2011) suggested that, if the photosphere of LS IV $-14^\circ 116$ is chemically stratified and pulsating, differential motion could be detected by comparing the radial velocity curves due to different elements. As a consequence, we have attempted over several years to resolve the surface motion of LS IV $-14^\circ 116$. This paper describes the observations attempted and the ultimate detection of surface motion associated with the principal photometric oscillation at a period of ~ 1950 s.

2 OBSERVATIONS

Spectroscopic time-series observations of LS IV $-14^\circ 116$ were obtained in 2005 with the Intermediate dispersion Spectrograph and Imaging System (ISIS) on the William Herschel Telescope (WHT), in 2005 with the University College Echelle Spectrograph (UCLES) of the Anglo-Australian Telescope (AAT), in 2007 with the **Cassegrain Grating Spectrograph (CGS)** on the 1.9 m telescope of the South African Astronomical Observatory (SAAO 1.9), in 2010 with the Wide-Field Spectrograph (WiFeS) on the Australian National University 2.3 m telescope (ANU 2.3), and in 2011 with the Ultraviolet and Visual Echelle Spectrograph (UVES) on the Very Large Telescope (VLT) of the European Southern Observatory (ESO). Details of dates observed, duration of observations in UT, wavelength range covered $\lambda\lambda$, spectral resolution R , exposure times t_{exp} , numbers of exposures n_{exp} , and average signal-to-noise ratio per exposure $\langle S/N \rangle$ are given in Table 1. The spectra were reduced using standard procedures, including bias-subtraction, flat-fielding, sky-subtraction, wavelength-calibration, and rectification. For UVES, the ESO pipeline reduced data were recovered from the ESO archive.

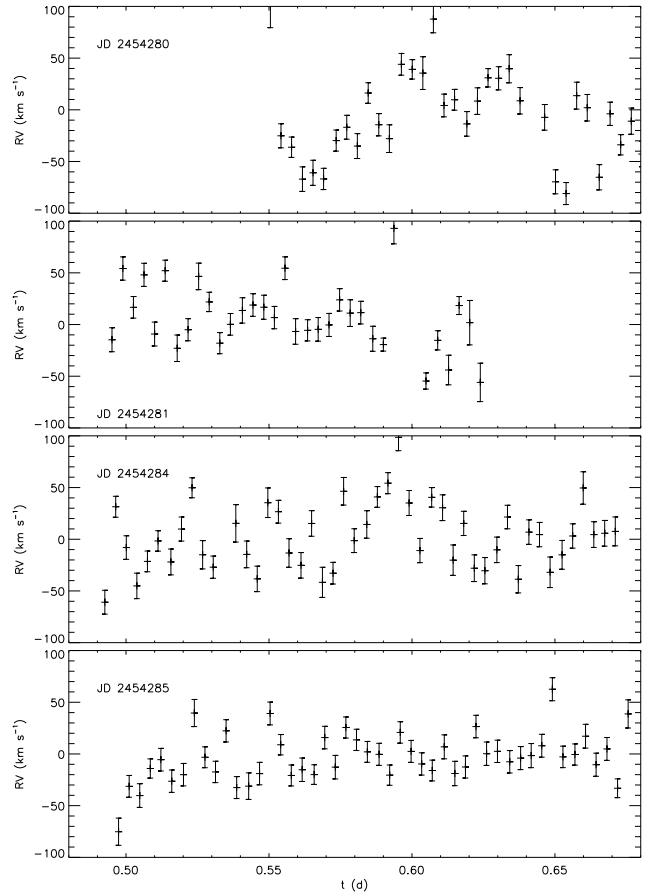


Figure 2. Relative radial velocities for LS IV $-14^\circ 116$ obtained with SAAO 1.9/CGS on 2007 June 29 - July 04.

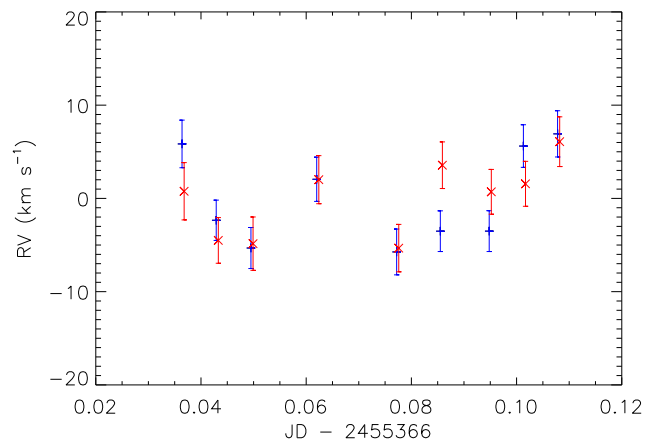


Figure 3. Relative radial velocities for LS IV $-14^\circ 116$ obtained with ANU 2.3/WiFeS on 2010 June 18 (blue '+' 420–488 nm, red 'x' 490–550 nm – offset by ± 0.0002 d for clarity).

3 VELOCITY MEASUREMENTS

Radial velocities were measured by cross-correlating each spectrum with a template defined to be a mean of all spectra for a given observing sequence. For this purpose, each spectrum was normalised to an approximate continuum, which was then subtracted. Cross-correlation was carried out in log wavelength space. Velocities were measured by fitting

Table 1. Observing log.

Telescope / Instrument	Date	UT _{start} – UT _{end}	λ nm	R	t_{exp} s	n_{exp}	$\langle S/N \rangle$	$\langle v_T \rangle$ km s ^{−1}	Observer
WHT/ISIS	2005 May 27	03:30 – 05:00	436–507	10 000	300	8	100	-153 ± 1	Ahmad
WHT/ISIS	2005 May 28	04:20 – 05:00	376–452	9 000	45	32	15–40	-153 ± 1	Ahmad
AAT/UCLES ¹	2005 Aug 27	11:41 – 13:30	382–521	30 000	1800	3	40	-153 ± 1	Ahmad
SAAO 1.9/CGS	2007 June 29	01:03 – 04:15	380–560	2 000	300	36	20–30	(-184 ± 10)	Ahmad
SAAO 1.9/CGS	2007 June 29–30	23:43 – 02:54	"	2 000	"	36	"	"	Ahmad
SAAO 1.9/CGS	2007 July 02–03	23:39 – 03:56	"	2 000	"	48	"	"	Ahmad
SAAO 1.9/CGS	2007 July 03–04	23:46 – 04:03	"	2 000	"	48	"	"	Ahmad
ANU 2.3/WiFES	2010 June 18	12:42 – 14:33	418–552	5 000	480	9	100	(-137 ± 3)	Kerzendorf
VLT/UVES	2011 Sept 07	02:31 – 06:20	330–680	100 000	300	39	30–40	-155 ± 1	Service

1: Naslim et al. (2011)

a parabola to a region around the maximum of the cross-correlation function (ccf) and customized to each wavelength region studied. The formal error in the position of the parabola apex was adopted as representative of the velocity error.

The observer’s frame radial velocity of the template was obtained by cross-correlation with a theoretical spectrum computed for a hot subdwarf with atmospheric abundances of hydrogen and helium being 70% and 30% by number, solar abundances of other elements, effective temperature $T_{\text{eff}} = 32\,000$ K, surface gravity $\log g = 5.5$ (cm s^{−2}), and microturbulent velocity $v_t = 5$ km s^{−1} (Behara & Jeffery 2006). This is not a perfect match to the observed spectrum, but completely satisfactory for the purpose of velocity measurement by cross correlation. Corrections to the heliocentric frame were then applied. These template velocities (v_T) are shown in Table 1. Because of uncertainty in the absolute wavelength calibration, the template velocities for the low-resolution data ($R < 6\,000$) are untrustworthy and are shown in parentheses. The *relative* velocities are much more reliable.

3.1 Radial Velocities

Relative velocities for the three individual AAT observations are not shown since the exposure times were long compared with the photometric variation.

The short duration of the WHT observations and the resolution of the SAAO observations were inadequate to offer any prospect of detecting the pulsation at 0.022 d, and show no evidence for longer-period variations (Figs. 1,2). Periodograms for these data showed no evidence of periodicity.

The WiFES data are divided into two wavelength regions (418 – 488 nm and 490 – 552 nm). Each was studied separately. Results are shown in Fig. 3. In general the two sets of velocities agree to within 2σ , where $\langle \sigma \rangle \approx 2.5$ km s^{−1}. There is little evidence for variability in excess of ± 5 km s^{−1} on a timescale of 0.1 d

The UVES data were recorded in three wavelength regions (330–452, 480–575, and 583–680 nm). These regions include broad Balmer, He I and He II lines. They include sharp stellar absorption lines from both light and heavy ions. They also include sharp interstellar and telluric absorption lines; there may also be residual instrumental artefacts. The latter all produce a sharp and stationary component in the ccf. The telluric absorption lines give an essentially flat velocity curve

with a maximum deviation of ± 2 km s^{−1} ($\langle \sigma \rangle \approx 0.25$ km s^{−1}) (Fig. 4). These velocities are consistent with small drifts in the instrumental calibration. The stellar absorption behaves quite differently and shows significant variability with a full amplitude of up to 15 km s^{−1} (Fig. 4). Although there are differences between velocities measured in different spectral regions and from different lines, the shape of the velocity curve is maintained. Therefore *we conclude the velocity curve to be real and due to variable motion of the stellar surface in the line of sight.*

The mean heliocentric radial velocity of LS IV −14°116 is -154 ± 1 km s^{−1}. This is large, but not unusual for a hot subdwarf in the thick disk. We see no evidence for long-period or large-amplitude variability that might suggest motion within a binary system.

3.2 Period

For each set of velocities measured from the UVES data, we computed the classical Fourier power spectrum and measured the frequency and semi-amplitude (as square root of power) of the highest peak (Fig. 5, Table 2). Owing to the short duration of the data series, ($T = 0.155$ d), the frequency resolution is low ($\Delta f = 1/T = 6.5$ d^{−1}). However, the frequency of the highest peak is clearly consistent with that of the largest-amplitude oscillation in the photometry of both Green et al. (2011) and Jeffery (2011). All lines for which a good solution was obtained yielded the same frequency (43.8 d^{−1}). The phases were the same to within ± 0.02 cycles.

Figure 6 shows the radial velocities for one line (He I 501.6 nm) phased on the dominant period (0.023 d). There remains substantial scatter about the best-fit sine curve, in excess of the formal errors on the velocities. Given the agreement between velocities obtained at different wavelengths, and the stability of the telluric velocity data, there is no reason to consider the errors to be seriously underestimated. We posit that *there is unresolved motion due to oscillations at other periods* as indicated by photometry.

3.3 Amplitude

It became clear that the amplitude of the velocity variation a_{RV} is sensitive to the wavelength window selected for cross-

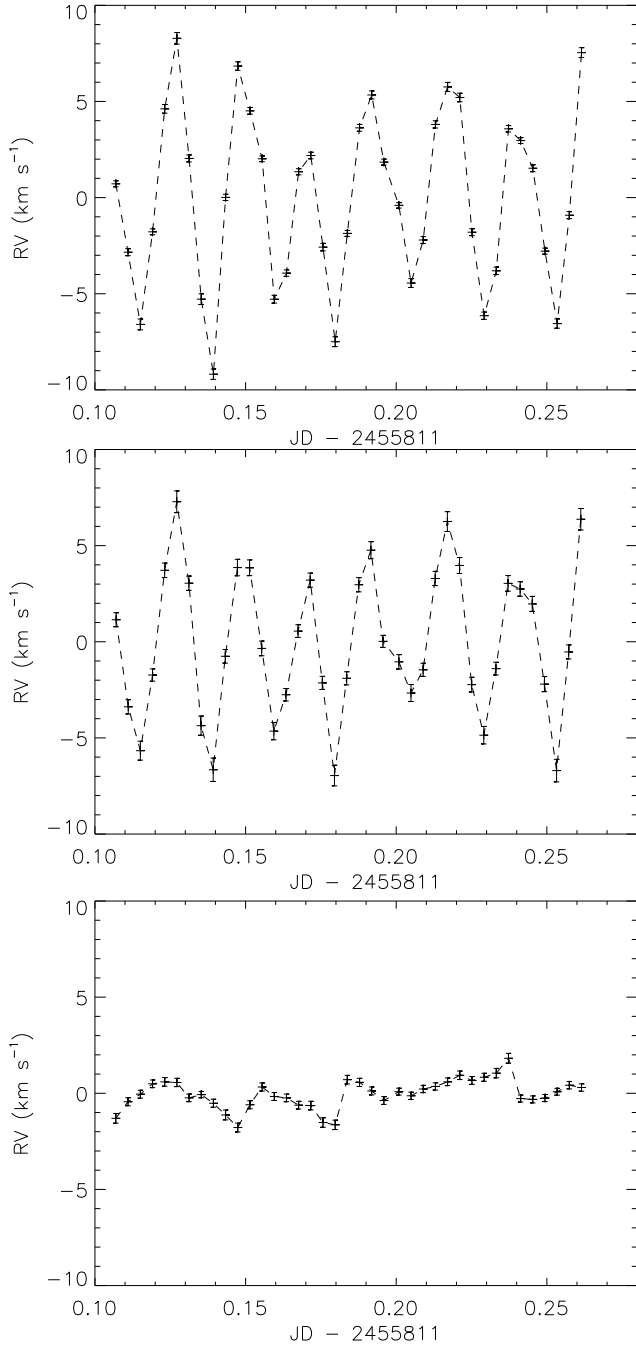


Figure 4. Relative radial velocities for LSIV $-14^{\circ}116$ obtained with VLT/UVES from 2011 Sept 07 for three different wavelength regions. Top: He I 501.6 nm. Middle: ‘metal’ absorption lines. Bottom: 627.0–632.5 nm telluric absorption lines. Since the sampling rate is quite low, data points are connected in order to guide the eye.

correlation (Table 2). The presence of interstellar lines or instrumental artefacts was indicated by a small sharp peak in the ccf, but by fitting the ccf peak over a large enough window, this was not a significant factor. Large spectral windows including many broad lines (*e.g.* 332–452 nm) would give small amplitudes, more restricted windows containing only sharp metal lines would give larger amplitudes (*e.g.*

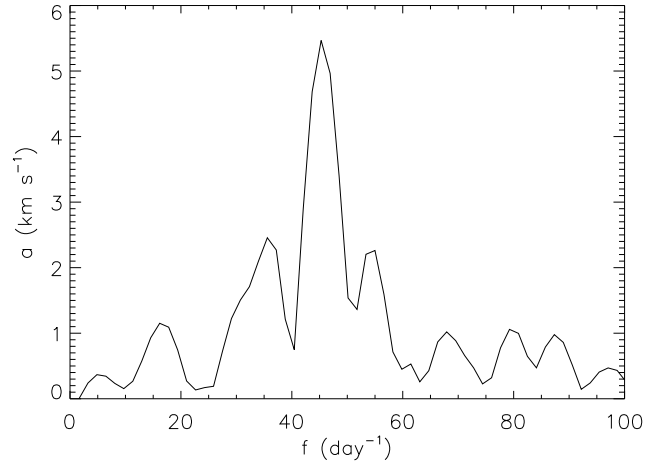


Figure 5. Classical power spectrum for radial velocities obtained from the He I 501.6 nm line observed with VLT/UVES on 2011 Sept 07.

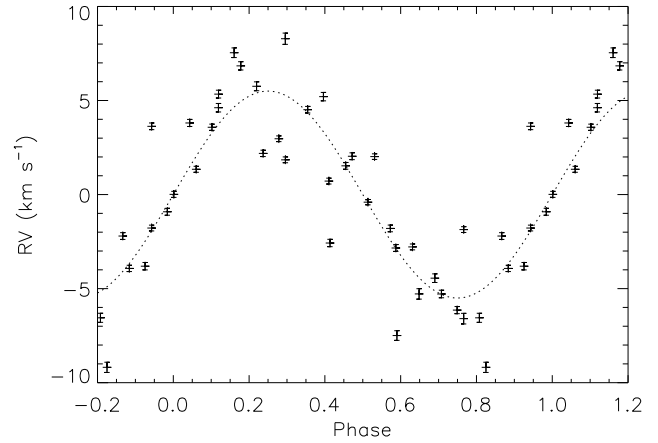


Figure 6. Radial velocity curve for LSIV $-14^{\circ}116$ obtained from the He I 501.6 nm line phased to the principal period of 1978 s with a semi-amplitude of 5.5 km s^{-1} .

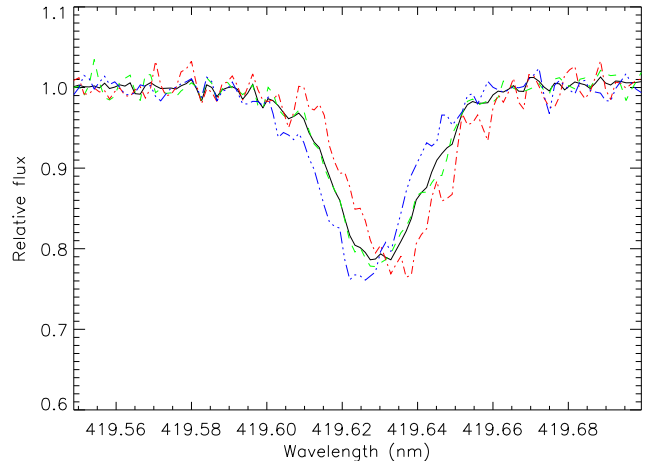
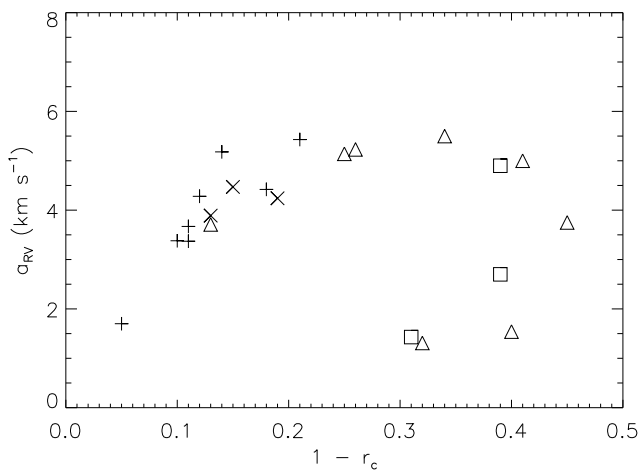


Figure 7. Zr IV line profiles for LSIV $-14^{\circ}116$ obtained from the mean spectrum (solid – black), around minimum (dot-dot-dot-dashed – blue: $v < -5 \text{ km s}^{-1}$), mean (dashed – green: $|v| < 1 \text{ km s}^{-1}$) and maximum (dot-dashed – red: $v > +5 \text{ km s}^{-1}$) relative radial velocity.

Table 2. Frequencies (f), velocity amplitudes (a_{RV}) and residual intensity at line centre (r_c) for various wavelength windows (λ).

Lines nm	λ nm	f d ⁻¹	a_{RV} km s ⁻¹	r_c	$\langle\sigma_{RV}\rangle$ km s ⁻¹
metals	415.5 – 430.0	43.8	4.6		
many	490.5 – 570.0	43.7	4.1		
many	332.0 – 452.0	43.7	2.7		
Sr II 407.8	407.5 – 407.8	43.8	3.4	0.90	0.33
Sr II 421.5	421.2 – 421.6	43.8	4.3	0.88	0.32
Ge II 417.9	417.5 – 417.9	43.8	5.2	0.86	0.33
Ge II 426.1	425.7 – 426.0	43.8	3.7	0.89	0.32
Ge II 429.1	428.6 – 429.2	43.8	1.7	0.95	0.37
Y III 404.0	403.6 – 4.3.9	43.8	3.4	0.89	0.31
Zr IV 413.7	413.4 – 413.7	45.4	2.8	0.89	0.43
Zr IV 419.8	419.5 – 419.7	43.8	5.4	0.79	0.16
Zr IV 431.7	431.3 – 431.7	43.8	4.4	0.82	0.23
C II 426.7	426.0 – 427.0	43.8	4.2	0.74	0.25
C III×3	406.3 – 407.0	43.8	3.9	0.87	0.25
N II 399.5	399.1 – 399.5	43.8	4.5	0.85	0.28
He I 386.7	386.3 – 386.8	43.8	3.7	0.87	0.79
He I 388.8	388.5 – 389.0	43.8	1.5	0.60	0.34
He I 396.3	396.0 – 396.5	43.8	1.3	0.68	0.22
He I 412.1	411.6 – 412.2	43.8	5.1	0.75	0.77
He I 438.8	438.0 – 439.3	43.8	5.2	0.74	1.63
He I 447.1	445.0 – 449.0	43.8	3.8	0.55	1.41
He I 501.6	500.0 – 502.5	43.8	5.5	0.66	0.20
He I 667.8	666.0 – 669.0	43.8	5.0	0.59	0.47
H α	655.5 – 656.5	45.3	1.4	0.69	1.63
H β	484.0 – 488.0	43.7	4.9	0.61	1.12
H γ	432.0 – 435.5	43.7	2.7	0.60	1.77
telluric	627.0 – 632.5	34	0.3	0.75	
$\langle\sigma\rangle$		6.5	0.1	0.01	


Figure 8. Radial velocity amplitude as a function of line depth. Symbols represent different elements: Sr, Ge, Y and Zr (+), C and N (x), He (Δ) and H (\square).

415–430 nm), whilst some individual lines would yield still larger amplitudes (*e.g.* He I 501.6 nm, Zr IV 419.8 nm).

For these UVES data, the cross-correlation approach yields high quality radial velocity information from individual lines in which the central depth r_c is at least 5% below continuum. Results for selected lines are shown in Table 2,

which also includes the mean velocity error ($\langle\sigma_{RV}\rangle$) for each line measured. There is a general trend that, for sharp lines, the velocity amplitude increases with line depth (Fig. 8).

For broad lines, especially the Balmer series and the diffuse He I lines, the amplitudes were frequently much lower ($\approx 1 - 2$ km s⁻¹), principally because the ccf peak is also very broad and therefore poorly defined. However, the same period of 0.023 d was generally recovered, except in the case of the Balmer lines.

One interpretation of the increase in velocity amplitude with central depth is that the pulsation amplitude is a function of position in the stellar atmosphere. Strong lines are formed at lower optical depths and, hence, higher in the atmosphere where densities are lower. An outward running wave will increase in amplitude as it propagates into less dense material, exactly as is observed in the sharp metal lines. Similar phenomena are seen, for example, in rapidly-oscillating Ap stars (Kurtz et al. 2007). In the case of LS IV-14°116 the situation is complicated by the apparent super-abundances of zirconium, strontium, etc., since it has been argued that the atmosphere must be chemically stratified. More detailed analysis of these and similar data should enable us to establish the relative depth of the chemically stratified layers relative to the velocity gradient in the photosphere.

3.4 Line Profiles

For large-amplitude radially pulsating stars, velocity shifts are usually associated with line-profile shifts; owing to the centre-to-limb contrast in radial velocity, there is usually some absorption at zero-velocity, whilst the line centre shifts back and forth producing asymmetric profiles at minimum and maximum radial velocity (Montañés Rodríguez & Jeffery 2001; Jeffery et al. 2013). Non-radial pulsations are often associated with line-profile variations, but usually in rapidly-rotating stars where temperature variations across the surface produce more or less flux at different velocities. We checked for line profile changes by coadding spectra around minimum velocity ($\delta v < -5$ km s⁻¹), mean velocity ($-1 < \delta v < +1$ km s⁻¹) and maximum velocity ($\delta v > 5$ km s⁻¹). No asymmetries were identified (*cf.* Fig. 7).

The use of a ccf template constructed as a simple mean allows for the possibility of some velocity smearing. In addition, the AAT/UCLES spectra used previously for atmospheric analysis were obtained with long exposures (*cf.* Naslim et al. (2011)). The question arises whether either the template could be sharpened, or whether previous analyses overlooked pulsation-broadening of the line profiles that led to an overestimate of the rotational broadening. We found no evidence that the spectrum of LS IV-14°116 could be further sharpened (Fig. 7), or that the (Naslim et al. 2011) measurement of $v \sin i < 2$ km s⁻¹ should be revised downward.

3.5 Light – velocity amplitude ratio

Green et al. (2011); Jeffery (2011) give the amplitude of the light variation in the optical as 0.27% or $\delta V \approx 3$ mmag. Taking the maximum amplitude of the radial velocity am-

plitude to be $\delta v \approx 6 \text{ km s}^{-1}$, the ratio of the observed light-amplitude to velocity amplitude in $\text{mmag km}^{-1} \text{ s}$ is thus $\delta V/\delta v \approx 0.5$. This ratio assumes that the amplitude of the 1953 s oscillation does not vary significantly over time.

We can simulate the observable light and amplitude ratios for non-radial modes of different radial degree ℓ and azimuthal number m using the surface codes BRUCE and KYLIE (Townsend 2003; Ramachandran et al. 2004) and a grid of theoretical spectra for a composition appropriate to LSIV $-14^\circ 116$ (Behara & Jeffery 2006; Naslim et al. 2011). Assuming effective temperature $T_{\text{eff}} = 36\,000 \text{ K}$, surface gravity $\log g = 5.6 (\text{cm s}^{-2})$ and equatorial rotation velocity $v_{\text{eq}} = 2 \text{ km s}^{-1}$ (Naslim et al. 2011), and **also assuming the adiabatic approximation**, a polar radius of $0.2 R_\odot$ (implying a mass $M \approx 0.5 M_\odot$), inclination $i = 80^\circ$, pulsation period 1950 s and an arbitrary surface velocity amplitude, we can compute a time series of theoretical spectra for a given mode ℓ, m . These can be analysed in exactly the same way as the UVES spectra to give both the apparent velocity amplitude and, also, the apparent flux amplitude in a given wavelength region. The ratio of surface velocity to apparent velocity amplitude is a function of ℓ, m and i , so we cannot infer anything directly from δv . However, the ratio $\delta V/\delta v$ is relatively invariant to i (Stamford & Watson 1981) and also to the surface velocity amplitude.

We computed theoretical $\delta V/\delta v$ for $\ell = 0, 1, 2$ and $m = 0, \dots, \ell$ for the dominant mode in LSIV $-14^\circ 116$, obtaining $\delta V/\delta v \approx 2 \text{ mmag km}^{-1} \text{ s}$ for the radial mode $\ell = 0$ and $\delta V/\delta v \approx 0.5 - 0.6 \text{ mmag km}^{-1} \text{ s}$ for the non-radial $\ell = 1$ and $\ell = 2$ modes. This *strongly argues against* the 1953 s period being a radial mode, in complete agreement with the argument from pulsation theory given by Green et al. (2011).

4 CONCLUSIONS

We have conducted a search for radial velocity variability in the helium-rich hot subdwarf LSIV $-14^\circ 116$: the pulsating zirconium star.

We have demonstrated that at least one periodic variation identified photometrically in LSIV $-14^\circ 116$ is also observable as a radial velocity variation with a semi-amplitude in excess of 5 km s^{-1} . This provides strong evidence that both are due to an oscillatory motion of the surface and are hence most likely due to pulsation. That is a purely empirical conclusion. Additional evidence from the light/velocity amplitude ratio argues that the pulsation cannot be a radial mode, whilst supporting arguments from pulsation theory (Green et al. 2011) confirm that the observed pulsations are due to a non-radial gravity mode.

We have also demonstrated that differential motion within the photosphere can be resolved by studying lines of different depths, as these probe different levels of the photosphere.

To learn more about LSIV $-14^\circ 116$ from these oscillations, the radial velocity measurements must be repeated over a longer period of time, and should be supported by multi-wavelength photometry. Higher frequency resolution would allow the relative phases of different lines to be measured and show how the oscillation propagates through the photosphere. Ultraviolet spectrophotometry would help to

identify the modes of oscillation, as well as to address the effective temperature question. Theoretical models need to be developed to interpret the spectrum, incorporating the non-radial oscillations, chemical stratification, and including differential vertical motion. In particular, the profiles and behaviour of the He I and hydrogen Balmer lines deserve further study.

ACKNOWLEDGMENTS

The Armagh Observatory is funded by direct grant-in-aid from the Northern Ireland Dept of Culture, Arts and Leisure. Observing travel for AA was funded by a PPARC grant. CSJ is indebted to Suzanna Randall for encouraging him to complete this study.

REFERENCES

- Ahmad A., Jeffery C. S., 2003, A&A, 402, 335
- Ahmad A., Jeffery C. S., 2004, Ap&SS, 291, 253
- Ahmad A., Jeffery C. S., 2005, A&A, 437, L51
- Behara N. T., Jeffery C. S., 2006, A&A, 451, 643
- Green E. M., Guvenen B., O'Malley C. J., O'Connell C. J., Baringer B. P., Villareal A. S., Carleton T. M., Fontaine G., Brassard P., Charpinet S., 2011, ApJ, 734, 59
- Jeffery C. S., 2011, Information Bulletin on Variable Stars, 5964, 1
- Jeffery C. S., Saio H., 2006, MNRAS, 371, 659
- Jeffery C. S., Saio H., 2007, MNRAS, 378, 379
- Jeffery C. S., Shibahashi H., Kurtz D. W., Elkin V., Montañés-Rodríguez P., Saio H., 2013, in Shibahashi H., Lynas-Gray A. E., eds, Astronomical Society of the Pacific Conference Series Vol. 479 of Astronomical Society of the Pacific Conference Series, Establishing Shock Diagnostics in the Pulsating Extreme Helium Star V652 Herculis. p. 369
- Kurtz D. W., Elkin V. G., Mathys G., van Wyk F., 2007, MNRAS, 381, 1301
- Miller Bertolami M. M., Córscico A. H., Althaus L. G., 2011, ApJ, 741, L3+
- Miller Bertolami M. M., Córscico A. H., Zhang X., Althaus L. G., Jeffery C. S., 2012, ArXiv e-prints
- Montañés Rodríguez P., Jeffery C. S., 2001, A&A, 375, 411
- Naslim N., Jeffery C. S., Behara N. T., Hibbert A., 2011, MNRAS, 412, 363
- Naslim N., Jeffery C. S., Hibbert A., Behara N. T., 2013, Monthly Notices of the Royal Astronomical Society, 434, 1920
- Ramachandran B., Jeffery C. S., Townsend R. H. D., 2004, A&A, 428, 209
- Stamford P. A., Watson R. D., 1981, Ap&SS, 77, 131
- Townsend R. H. D., 2003, MNRAS, 343, 863
- Townsend R. H. D., Owocki S. P., Groote D., 2005, ApJ, 630, L81
- Viton M., Deleuil M., Tobin W., Prevot L., Bouchet P., 1991, A&A, 242, 175